



Dipartimento di Elettronica e Informazione e Bioingegneria

**Politecnico  
di Milano**

20133 Milano (Italia)  
Piazza Leonardo da Vinci, 32  
Tel. (39) 02-2399.3400  
Fax (39) 02-2399.7680

## **Arrays of First-Order Steerable Differential Microphones**

F. Borra, A. Bernardini, I. Bertuletti, F. Antonacci, A. Sarti, "Arrays of First-Order Steerable Differential Microphones" in Proc. *IEEE International Conference on Acoustics Speech and Signal Processing (ICASSP) 2021*

**Published in:**

Proceedings of *IEEE International Conference on Acoustics Speech and Signal Processing (ICASSP) 2021*

**Document Version:**

Postprint version

**Publisher rights:**

© 2021 IEEE. This work is made available online in accordance with the publisher's policies. Please refer to any applicable terms of use of the publisher.

**Note:**

This version of the article contains corrections of typos present in the published version. A list of such corrections is reported at the end of this file.

# ARRAYS OF FIRST-ORDER STEERABLE DIFFERENTIAL MICROPHONES

Federico Borra, Alberto Bernardini, Ivan Bertuletti, Fabio Antonacci, Augusto Sarti

Dipartimento di Elettronica, Informazione e Bioingegneria,  
Politecnico di Milano, Piazza L. Da Vinci 32, 20133 Milano, Italy

## ABSTRACT

The literature is rich with techniques for the design of small-size Differential Microphone Arrays (DMAs), known for their almost frequency-invariant beampatterns and low computational cost. Few works, instead, discuss the properties of beamformers based on multiple DMA units. In this paper, we consider arbitrarily shaped planar arrays of DMA units. In turn, each DMA unit is a first-order continuously-steerable differential microphone characterized by an arbitrary configuration of omnidirectional sensors and a symmetric beampattern. We present a beamforming technique that, assumed all the DMA units to steer identical beams in the same direction, allows us to approach the behavior of a Delay-And-Sum beamformer or Super-Directive beamformer by solely varying a single scalar parameter. Efficient implementations of the proposed beamformers can be developed by taking into account that, for a wide range of frequencies, the values of such a parameter are practically invariant with respect to the geometry of the array.

**Index Terms**— Microphone Arrays, Differential Beamforming

## 1. INTRODUCTION

In the recent years, several research works focused on the development of strategies for the design of small-size Differential Microphone Arrays (DMAs) [1–8] because of their nearly frequency-invariant beampattern, good directivity properties and low computational cost. Spatial responses of DMAs can be designed to match beampatterns of arbitrary order, even though low-order (especially first-order) DMAs are usually preferred in practice [1, 2, 9, 10]. In fact, DMAs are affected by white noise amplification at low frequencies, high sensitivity to misplacements of omnidirectional sensors and gain or phase mismatches all the more as the order is increased [3, 11, 12].

Most DMAs in the literature are characterized by linear or circular array geometries [7, 13–18]; however, in [19] a generalized approach for the frequency domain design of DMAs with arbitrary geometry and arbitrary order is presented. Starting from the results in [19], highly efficient frequency domain and discrete-time domain methods, essentially based on the linear combination of first-order eigenbeams, are introduced in [20] for the implementation of steerable first-order DMAs with arbitrary geometry. Although the literature is rich with works regarding the design of small-size DMAs, few publications discuss the properties of beamformers made of multiple *DMA units* [21, 22]. A first step in this research direction is made in [21] where a beamforming technique based on a two-stage filtering approach is applied to a uniform linear array of first-order steerable DMA units, each composed of four omnidirectional sensors. The first stage is the local filtering performed by the DMA units (that are assumed to steer identical beams in the same direction); the second stage is a delay-and-sum beamformer applied to the *virtual*

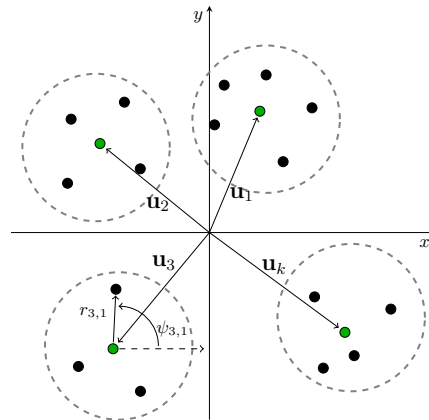


**Fig. 1:** Example of planar array of DMA units. Green dots indicate the reference points of the DMA units.

array (i.e., the array whose steering vector refers to the reference-points of the DMA units). The resulting global beamformer can efficiently morph between a Delay-And-Sum-like beamformer and a Super-Directive-like beamformer just by varying a scalar parameter that determines the shape of the first-order beams. Moreover, no matrix inversion is needed for deriving the filters. A technique similar to the one in [21] is discussed in [22] where Kronecker product beamforming is applied to arbitrary arrays of identical DMA units.

In this paper, we extend the approach presented in [21] by considering configurations of sensors with both arbitrary geometry of the DMA unit and arbitrary geometry of the virtual array. We solve optimization problems to derive the first-order beam parameters that maximize the White Noise Gain (WNG) and the Directivity Factor (DF) of the global beamformer. We show that the derived optimal parameters are nearly invariant w.r.t. the considered array geometry. This fact makes the design of the proposed class of beamformers extremely simple, with no need of matrix inversion for implementing the filters. Even more efficient beamformers can be achieved by combining the implementation strategies discussed in [20, 21] with the proposed approach, paving the way towards computationally inexpensive discrete-time realizations of spatial filters characterized by arbitrary arrays of DMA units.

## 2. SIGNAL MODELS AND METRICS

Let us consider a planar array consisting of  $K$  DMA units, each one having a potentially different number of sensors  $M_k$ , with index  $k \in \{1, \dots, K\}$ . Both the geometry of the DMA units and of the virtual array are arbitrary. Fig. 1 shows a configuration example, where each green dot identifies the *reference point* of each DMA

unit (we conventionally consider the center of mass).

### 2.1. DMA Unit Signal Model

Under the far-field assumption, the propagation vector of a plane-wave impinging the  $k$ th DMA unit from the azimuth direction  $\theta$  is [19, 20]

$$\mathbf{d}_k(\omega, \theta) = \left[ e^{j\bar{\omega}_{k,1} \cos(\theta - \psi_{k,1})}, \dots, e^{j\bar{\omega}_{k,M_k} \cos(\theta - \psi_{k,M_k})} \right]^T \quad (1)$$

where  $j$  is the imaginary unit,  $\bar{\omega}_{k,m} = \omega r_{k,m}/c$  with  $\omega = 2\pi f$  the angular frequency,  $f > 0$  the temporal frequency,  $c$  the speed of sound, while  $r_{k,m}$  and  $\psi_{k,m}$  are the distance and the angular position of the  $m$ th microphone (with  $m \in \{1, \dots, M_k\}$ ) in the  $k$ th DMA unit w.r.t. its reference point, respectively. The signal sensed by the  $k$ th DMA unit can be modelled as [19, 20]

$$\mathbf{y}_k(\omega) = \mathbf{d}_k(\omega, \theta)X_k(\omega) + \mathbf{v}_k(\omega), \quad (2)$$

where  $X_k(\omega)$  is the source signal at the reference point of the  $k$ th DMA unit and the vector  $\mathbf{v}_k(\omega)$  models an additive noise. The signal  $\mathbf{y}_k(\omega)$  is processed with a filter  $\mathbf{w}_k(\omega)$  according to

$$Z_k(\omega) = \mathbf{w}_k^H(\omega)\mathbf{y}_k(\omega), \quad (3)$$

where  $(\cdot)^H$  is the conjugate-transpose operator.

### 2.2. Global Array Signal Model

We define  $\mathbf{u}_k = [u_{k,x}, u_{k,y}]^T$  as the vector containing the spatial coordinates of the reference point of the  $k$ th DMA unit, as indicated in Fig. 1. Under the far-field assumption, the propagation vector of a plane-wave impinging the virtual array from direction  $\theta$ , taking as a reference the center of the coordinate axes, is

$$\mathbf{a}(\omega, \theta) = \left[ e^{j\omega \frac{u_{1,x} \cos \theta + u_{1,y} \sin \theta}{c}}, \dots, e^{j\omega \frac{u_{K,x} \cos \theta + u_{K,y} \sin \theta}{c}} \right]^T. \quad (4)$$

We can write the signal model of the *global array* by combining (1) and (4) as

$$\mathbf{y}(\omega) = \mathbf{d}(\omega, \theta)X(\omega) + \mathbf{v}(\omega), \quad (5)$$

where

$$\mathbf{y}(\omega) = [\mathbf{y}_1^T(\omega), \dots, \mathbf{y}_K^T(\omega)]^T, \quad \mathbf{v}(\omega) = [\mathbf{v}_1^T(\omega), \dots, \mathbf{v}_K^T(\omega)]^T, \\ \mathbf{d}(\omega, \theta) = \text{diag}(\mathbf{d}_1(\omega, \theta), \dots, \mathbf{d}_K(\omega, \theta)) \mathbf{a}(\omega, \theta)$$

with  $\text{diag}(\cdot)$  the operator that builds a block-diagonal matrix with the list of matrices in the argument and  $X(\omega)$  is the desired signal at the center of the coordinate axes. The filtering process of the global array is expressed as

$$\bar{Z}(\omega) = \mathbf{g}^H(\omega)\mathbf{y}(\omega). \quad (6)$$

where  $\mathbf{g}(\omega)$  is here called the *global array filter*<sup>1</sup> and can be conveniently decomposed as follows

$$\mathbf{g}(\omega) = \text{diag}(\mathbf{w}_1(\omega), \dots, \mathbf{w}_K(\omega))\mathbf{h}(\omega), \quad (7)$$

where  $\mathbf{h}(\omega)$  will be referred to as virtual array filter. It is worth noticing that the expression of the global array filter based on a block diagonal matrix (7) used here is more general than the one based on the Kronecker product used in [22], since it allows us to describe virtual arrays with arbitrary geometry where also the DMA units can have arbitrary geometry and different numbers of sensors.

<sup>1</sup>We use the expression *global array filter* in the sense employed in [22] that differs from the sense used in [21] which, instead, refers to the filter called *virtual array filter* in this manuscript.

### 2.3. Metrics

Spatial filters are typically designed in such a way that they optimize a given metric. Two important metrics quantify the gain in Signal-to-Noise-Ratio (SNR) (i.e., the ratio between the output SNR and the input SNR) achieved by a beamformer. The first, called White Noise Gain (WNG) [5], is referred to spatially white noise,

$$\text{WNG}[\mathbf{g}(\omega)] = \frac{|\mathbf{g}^H(\omega)\mathbf{d}(\omega, \theta)|^2}{\mathbf{g}^H(\omega)\mathbf{g}(\omega)} \quad (8)$$

while the second, called Directivity Factor (DF) [5], is referred to diffuse noise with covariance matrix  $\mathbf{\Gamma}_{\text{dn}}(\omega)$ ,

$$\text{DF}[\mathbf{g}(\omega)] = \frac{|\mathbf{g}^H(\omega)\mathbf{d}(\omega, \theta)|^2}{\mathbf{g}^H(\omega)\mathbf{\Gamma}_{\text{dn}}(\omega)\mathbf{g}(\omega)}, \quad [\mathbf{\Gamma}_{\text{dn}}(\omega)]_{i,j} = \frac{\sin[\omega\rho_{ij}/c]}{\omega\rho_{ij}/c} \quad (9)$$

where  $\rho_{ij}$  is the Euclidean distance between the  $i$ th and the  $j$ th microphones. Another fundamental metric is the beampattern, i.e., the spatial response of the beamformer, expressed as a function of the direction of arrival  $\theta$  as [5]

$$\mathcal{B}[\mathbf{g}(\omega), \theta] = \mathbf{g}^H(\omega)\mathbf{d}(\omega, \theta). \quad (10)$$

## 3. TWO-STAGE BEAMFORMER DESIGN

In this section we describe the proposed approach to design the global array filter  $\mathbf{g}(\omega)$  in (7). First, we show the structure of the filter of each DMA unit  $\mathbf{w}_k(\omega)$  and the virtual array filter  $\mathbf{h}(\omega)$  and, then, we set up an optimization problem in order to find the optimal values of the free parameters that maximize the WNG and the DF.

### 3.1. DMA Unit Filter

As far as the local filters of the DMA units are concerned, we use the filtering approach proposed in [20] that enables efficient implementations of first-order steerable DMA units with arbitrary planar geometry. We thus define the  $k$ th DMA unit filter as

$$\mathbf{w}_k(\omega) = (1 - q)[\mathbf{P}_k]_{:,2} - q \frac{2c}{j\omega} \left( \Re \left\{ ([\mathbf{P}_k^*]_{:,1}) e^{j\theta} \right\} \right), \quad (11)$$

where the operator  $\Re\{\cdot\}$  returns the real part of a complex number,  $(\cdot)^*$  denotes complex conjugation and  $[\mathbf{P}_k^*]_{:,i}$  refers to the  $i$ th column of matrix  $\mathbf{P}_k^*$ , where  $\mathbf{P}_k$  is defined as

$$\mathbf{P}_k = \mathbf{\Phi}_k^H \left( \mathbf{\Phi}_k \mathbf{\Phi}_k^H \right)^{-1} \quad (12)$$

with

$$\mathbf{\Phi}_k = \begin{bmatrix} r_{k,1} e^{-j\psi_{k,1}} & r_{k,2} e^{-j\psi_{k,2}} & \dots & r_{k,M_k} e^{-j\psi_{k,M_k}} \\ 1 & 1 & \dots & 1 \\ r_{k,1} e^{j\psi_{k,1}} & r_{k,2} e^{j\psi_{k,2}} & \dots & r_{k,M_k} e^{j\psi_{k,M_k}} \end{bmatrix}.$$

The parameter  $q \in [0, 1]$  determines the shape of the beampattern of the DMA unit (e.g.,  $q = 0$  leads to an omnidirectional beampattern while  $q = 1$  to a dipole) while the parameter  $\theta \in [0, 2\pi)$  controls the steering direction of the beam. As in [21], we assume that all the  $K$  DMA units are characterized by the same beam steered to the same direction. Hence, the parameters  $q$  and  $\theta$  are equal for all DMA units. How to set the parameters  $q$  and  $\theta$  will be discussed in Sec. 3.3.

### 3.2. Virtual Array Filter

Similarly to what done in [21], as a virtual array filter, we decide to adopt a simple Delay-and-Sum (DAS) beamformer defined as

$$\mathbf{h}(\omega) = \frac{\mathbf{a}(\omega, \phi)}{\mathbf{a}(\omega, \phi)^H \mathbf{a}(\omega, \phi)}. \quad (13)$$

The only parameter to be designed for the virtual array beamformer is thus the steering direction  $\phi$ .

### 3.3. Optimization problems

According to the previous subsections, the three parameters to be set are: the DMA unit beam shape parameter  $q$ , the steering direction of the DMA units  $\theta$  and the one of the virtual array beamformer  $\phi$ . For the sake of convenience, we rewrite (7) by making explicit the dependence from such parameters

$$\begin{aligned} \mathbf{g}(\omega, q, \theta, \phi) &= \mathbf{H}(\omega, \phi) [(1-q)\mathbf{w}_o + q\mathbf{w}_d(\omega, \theta)] \\ &= q\mathbf{H}(\omega, \phi) [\mathbf{w}_d(\omega, \theta) - \mathbf{w}_o] + \mathbf{H}(\omega, \phi)\mathbf{w}_o \\ &= q\boldsymbol{\ell}(\omega, \theta, \phi) + \boldsymbol{\kappa}(\omega, \phi) \end{aligned} \quad (14)$$

where

$$\begin{aligned} \boldsymbol{\ell}(\omega, \theta, \phi) &= \mathbf{H}(\omega, \phi) [\mathbf{w}_d(\omega, \theta) - \mathbf{w}_o], \quad \boldsymbol{\kappa}(\omega, \phi) = \mathbf{H}(\omega, \phi)\mathbf{w}_o \\ \mathbf{H}(\omega, \phi) &= \text{diag}(H_1(\omega, \phi)\mathbf{I}_{M_1}, \dots, H_K(\omega, \phi)\mathbf{I}_{M_k}), \\ \mathbf{w}_o &= \left[ [\mathbf{P}_1]_{:,2}^T, \dots, [\mathbf{P}_K]_{:,2}^T \right]^T \\ \mathbf{w}_d(\omega, \theta) &= \frac{-2c}{j\omega} \left[ \Re \left\{ [\mathbf{P}_1]_{:,1}^H e^{j\theta} \right\}, \dots, \Re \left\{ [\mathbf{P}_K]_{:,1}^H e^{j\theta} \right\} \right]^T \end{aligned}$$

with  $\mathbf{I}_{M_k}$  the  $M_k \times M_k$  identity matrix and  $H_k(\omega, \phi)$  the  $k$ th element of vector  $\mathbf{h}(\omega)$  in (13).

In order to maximize the WNG and the DF, respectively, we minimize the denominator of the right-side expression of eq. (8) and eq. (9), by setting up the following optimization problem

$$\begin{aligned} \arg \min_{q, \theta, \phi} \quad & \mathbf{g}^H(\omega, q, \theta, \phi) \mathbf{R}(\omega) \mathbf{g}(\omega, q, \theta, \phi) \\ \text{subject to} \quad & \mathbf{w}_k^H(\omega, q, \theta) \mathbf{d}_k(\omega, \theta_s) = 1, \quad k = 1, \dots, K \\ & \mathbf{h}^H(\omega, \phi) \mathbf{a}(\omega, \theta_s) = 1 \\ & 0 \leq q \leq 1, \end{aligned} \quad (15)$$

where  $\theta_s$  is the desired steering direction of the global array beamformer,  $\mathbf{R}(\omega) = E[\mathbf{y}(\omega)\mathbf{y}^H(\omega)]$  is the noise covariance matrix and  $E[\cdot]$  the expectation operator. The first two constraints ensure a distortionless response in the desired direction  $\theta_s$ . It follows that the first can be easily satisfied by setting  $\theta = \theta_s$  in (11) while the second by setting  $\phi = \theta_s$  in (13). Since the only parameter left to be set is  $q$ , the optimization problem reduces to

$$\begin{aligned} \arg \min_q \quad & q^2 \boldsymbol{\ell}^H(\omega) \mathbf{R}(\omega) \boldsymbol{\ell}(\omega) + 2q \Re \{ \boldsymbol{\ell}^H(\omega) \mathbf{R}(\omega) \boldsymbol{\kappa}(\omega) \} \\ \text{subject to} \quad & 0 \leq q \leq 1 \end{aligned} \quad (16)$$

In the next section we show the optimal values of  $q$  both when we maximize the WNG, i.e.,  $\mathbf{R}(\omega) = \mathbf{I}$  where  $\mathbf{I}$  is the identity matrix, and the DF, i.e.,  $\mathbf{R}(\omega) = \boldsymbol{\Gamma}_{\text{dn}}(\omega)$ . The optimization problem in (16) provides a value of  $q$  that depends on the angular frequency  $\omega$ . However, it is well-known that the beampattern of small-sized arrays is nearly frequency-invariant [15, 17]. For this reason, we also

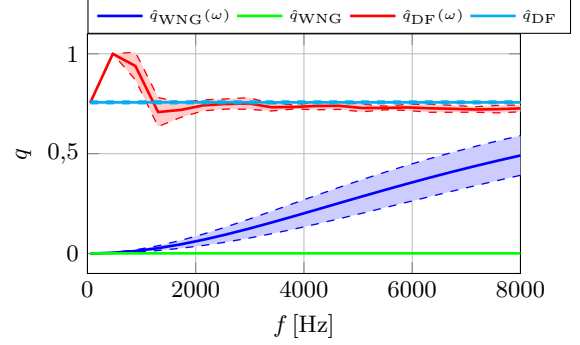


**Fig. 2:** Frequency-dependent and frequency-independent  $q$  as a function of frequency. Solid lines represent the mean while dashed lines the standard deviation over the  $G$  different tested geometries.

set up another an optimization problem in which  $q$  does not depend on frequency as

$$\begin{aligned} \arg \min_q \quad & q^2 \sum_{i=1}^N \boldsymbol{\ell}^H(\omega_i) \mathbf{R}(\omega_i) \boldsymbol{\ell}(\omega_i) + \\ & + 2q \sum_{i=1}^N \Re \{ \boldsymbol{\ell}^H(\omega_i) \mathbf{R}(\omega_i) \boldsymbol{\kappa}(\omega_i) \} \\ \text{subject to} \quad & 0 \leq q \leq 1, \end{aligned} \quad (17)$$

where  $\omega_1, \dots, \omega_N$  are uniformly distanced samples of the frequency axis.

## 4. STUDY ON ARRAY GEOMETRY

In this section we solve the frequency dependent (16) and the frequency independent (17) optimization problems in order to derive the values of the parameter  $q$  that maximize the WNG and the DF. We test  $G = 1000$  different array geometries characterized by  $K = 10$  DMA units, whose positions are identified by vectors  $\mathbf{u}_k$  as shown in Fig. 1. The chosen norms and angles of vectors  $\mathbf{u}_k$  are samples of the uniform distributions  $\|\mathbf{u}_k\| \sim \mathcal{U}(5 \text{ cm}, 25 \text{ cm})$  and  $\angle \mathbf{u}_k \sim \mathcal{U}(0, 2\pi)$ , respectively, where  $\mathcal{U}(a, b)$  generally indicates a uniform distribution with boundaries  $a$  and  $b$ . We constrain the reference points of the different DMA units to be at least 10 cm apart. The number  $M_k$  of omnidirectional sensors of each DMA unit is randomly chosen according to  $M_k \sim \mathcal{U}(4, 6)$ , while the positions of the sensors follows  $r_{k,m} \sim \mathcal{U}(0.3 \text{ cm}, 1.5 \text{ cm})$  and  $\psi_{k,m} \sim \mathcal{U}(0, 2\pi)$ . Also for the sensors in each DMA unit we constrain their positions to be at least 0.3 cm apart. For all the simulations we fix the desired steering direction  $\theta_s = 0^\circ$ .

Let us indicate with  $\hat{q}_{\text{WNG}}(\omega)$  and  $\hat{q}_{\text{WNG}}$  the solutions to (16) and (17), respectively, obtained by setting  $\mathbf{R}(\omega) = \mathbf{I}$  (WNG maximization cases). Similarly, we call  $\hat{q}_{\text{DF}}(\omega)$  and  $\hat{q}_{\text{DF}}$  the solutions obtained by setting  $\mathbf{R}(\omega) = \boldsymbol{\Gamma}_{\text{dn}}(\omega)$  (DF maximization cases). Fig. 2 shows the mean and the standard deviation of the optimal  $\hat{q}_{\text{WNG}}(\omega)$ ,  $\hat{q}_{\text{WNG}}$ ,  $\hat{q}_{\text{DF}}(\omega)$  and  $\hat{q}_{\text{DF}}$  as a function of frequency. As we can see, in the frequency-independent case, the standard deviation is lower than in the frequency-dependent case. The upper plot in Fig. 3 shows the mean and the standard deviation of the DF of the beamformers designed with the values of  $q$  reported in Fig. 2. Similarly to what done in [21], we also report the DF of single-stage DAS and SD

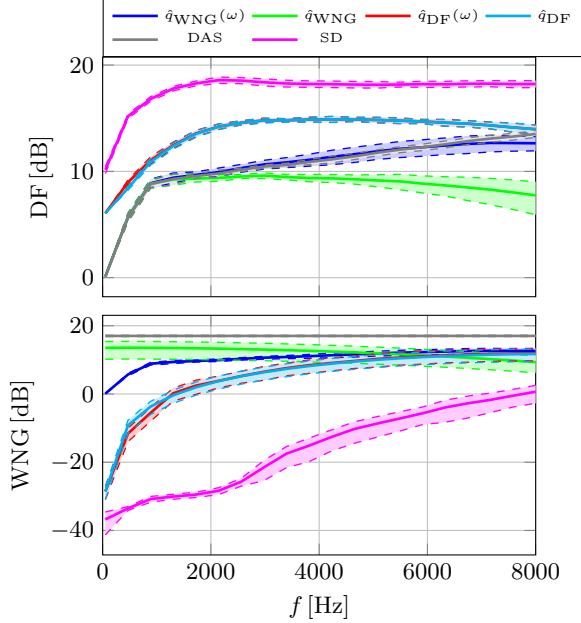


**Fig. 3:** Directivity Factor and White-Noise-Gain as a function of frequency. Solid lines represent the mean while dashed lines the standard deviation over the  $G$  different tested geometries.

beamformers (i.e., designed and optimized considering all the sensors of the global array at once [23]). We notice that spatial filters based on  $\hat{q}_{DF}(\omega)$  and  $\hat{q}_{DF}$  clearly exhibit an higher DF w.r.t. the ones using  $\hat{q}_{WNG}(\omega)$  and  $\hat{q}_{WNG}$ . Interestingly, filters obtained with  $\hat{q}_{DF}(\omega)$  and  $\hat{q}_{DF}$  are characterized by almost indistinguishable mean DF values at all frequencies and low standard deviation along the  $G$  different array geometries. Similar conclusions can be drawn for the lower plot in Fig. 3 showing the WNG; in this case, spatial beamformers obtained with  $\hat{q}_{WNG}(\omega)$  and  $\hat{q}_{WNG}$  do have a similar behavior and are characterized by an higher WNG than those characterized by  $\hat{q}_{DF}(\omega)$  and  $\hat{q}_{DF}$ . The left plot of Fig. 4 shows that the average spatial response of the proposed two-stage beamformer using  $\hat{q}_{WNG}$  highly matches the one of the single-stage DAS beamformers. The right plot of Fig. 4, instead, shows a comparison between the average beampattern obtained using the two-stage approach with  $\hat{q}_{DF}$  and a single-stage SD. Here we notice that the mainlobe of the two-stage beamformers is slightly larger w.r.t. the one of the single-stage SD. It is worth noticing that the proposed approach, however, is capable of morphing between DAS-like beamformers and SD-like beamformers by solely varying the  $q$  parameter (no matrix inversion is needed).

## 5. DISCRETE-TIME DOMAIN IMPLEMENTATION

As outlined in [16, 20, 24] discrete-time domain implementations of beamformers are, in certain application scenarios, e.g., embedded systems, preferred to frequency domain implementations because of their lower computational complexity and higher flexibility. In this regard, a discrete-time realization of the proposed beamformer can be designed starting from the implementation of the DMA unit discussed in [20], i.e.,

$$z_k[n] = (1 - q)z_{k,o}[n] + qz_{k,d}[n], \quad (18)$$

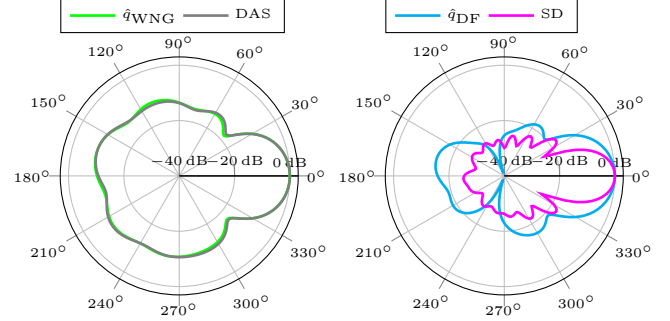


**Fig. 4:** Average beampattern at 1 kHz along the  $G$  different tested geometries. Maximum standard deviation are of 3.71 dB, 3.35 dB, 3.86 dB and 3.65 dB for the  $\hat{q}_{WNG}$ , DAS,  $\hat{q}_{DF}$  and SD, respectively.

where  $z_k[n]$  is the discrete-time version of  $Z_k(\omega)$ ,  $n$  being the sample index,  $q$  is assumed to be frequency independent,

$$\begin{aligned} z_{k,o}[n] &= [\mathbf{P}_k]_{:,2}^T \mathbf{y}_k[n] \\ z_{k,d}[n] &= \frac{c}{F_s} (y_{k,d}[n] + y_{k,d}[n-1]) + z_{k,d}[n-1] \end{aligned} \quad (19)$$

with  $F_s$  the sampling frequency,  $\mathbf{y}_k[n]$  a  $M_k \times 1$  vector of the  $k$ th DMA unit sensor signals and

$$y_{k,d}[n] = \Re\{[\mathbf{P}_k]_{:,1}^H e^{j\theta}\} \mathbf{y}_k[n]. \quad (20)$$

A discrete-time realization of the DAS virtual array filter  $\mathbf{h}(\omega)$  in (13), instead, can be obtained using fractional delay filters [25]. The output of the global array is therefore

$$\bar{z}[n] = \sum_{k=1}^K h_k[n] * z_k[n], \quad (21)$$

where  $*$  indicates convolution,  $\bar{z}[n]$  is the discrete-time version of  $\bar{Z}(\omega)$  and  $h_k[n]$  are the discrete-time coefficients of FIR filters implementing fractional delays [25].

According to (21) and (18), we can also express the output of the proposed beamformer as

$$\bar{z}[n] = (1 - q) \sum_{k=1}^K h_k[n] * z_{k,o}[n] + q \sum_{k=1}^K h_k[n] * z_{k,d}[n]. \quad (22)$$

Eq. (22) highlights the fact that, by simply adjusting the single scalar parameter  $q$ , we can efficiently vary the directivity of the global beamformer.

## 6. CONCLUSIONS

In this paper we presented a two-stage spatial filtering approach for arbitrary planar arrays of first-order steerable DMA units. We proposed a design methodology that, fixed the virtual array filter, optimizes the value of the beam shape parameter  $q$  of all DMA units in order to maximize either the WNG or the DF, both in a frequency-dependent and in a frequency-independent fashion. Frequency-dependent and frequency-independent optimum parameters exhibit very similar behaviour in terms of WNG and DF for a wide range of frequencies. Moreover, we showed that the behavior of the two-stage beamformer is nearly invariant w.r.t. the array geometry. We also discussed an efficient discrete-time domain implementation of the proposed two-stage filtering approach that allows us to morph between a DAS-like and a SD-like beamformer just by varying a single scalar parameter.

## 7. REFERENCES

- [1] G. W. Elko and A. T. N. Pong, "A steerable and variable first order differential microphone array," in *Proc. IEEE International Conference on Acoustics, Speech and Signal Processing (ICASSP)*, Apr. 1997, vol. 1.
- [2] H. Teutsch and G. W. Elko, "First- and second- order adaptive differential microphone arrays," in *Proc. IWAENC*, Sep. 2001, pp. 35–38.
- [3] M. Buck, "Aspects of first-order differential microphone arrays in the presence of sensor imperfections," *European Transactions on Telecommunications*, vol. 13, no. 1, pp. 115–122, Mar.-Apr. 2002.
- [4] G. W. Elko, "Differential microphone arrays," in *Audio Signal Processing for Next-Generation Multimedia Communication Systems*, Y. Huang and J. Benesty, MA: Kluwer Norwell, Ed., 2004.
- [5] J. Benesty and J. Chen, *Study and Design of Differential Microphone Arrays*, vol. 6, Springer Science & Business Media, 2013.
- [6] H. Zhang, J. Chen, and J. Benesty, "Study of nonuniform linear differential microphone arrays with the minimum-norm filter," *Applied Acoustics, Elsevier*, vol. 98, pp. 62–69, Nov 2015.
- [7] J. Benesty, J. Chen, and I. Cohen, *Design of Circular Differential Microphone Arrays*, vol. 12 of *Springer Topics in Signal Processing*, Springer International Publishing, Cham, 2015.
- [8] A. Bernardini, M. D'Aria, R. Sannino, and A. Sarti, "Efficient Continuous Beam Steering for Planar Arrays of Differential Microphones," *IEEE Signal Processing Letters*, vol. 24, no. 6, pp. 794–798, June 2017.
- [9] M. Buck and M. Rodler, "First order differential microphone arrays for automotive applications," in *Proc. IWAENC*, Sep. 2001, pp. 19–22.
- [10] Q. Tu and H. Chen, "Array configuration optimization of first-order steerable differential arrays with minimum number of microphones," *The Journal of the Acoustical Society of America*, vol. 148, no. 3, pp. 1732–1747, 2020.
- [11] X. Wu, H. Chen, J. Zhou, and T. Guo, "Study of the mainlobe misorientation of the first-order steerable differential array in the presence of microphone gain and phase errors," *IEEE Signal Processing Letters*, vol. 21, no. 6, pp. 667–671, June 2014.
- [12] X. Wu and H. Chen, "Directivity Factors of the First-Order Steerable Differential Array With Microphone Mismatches: Deterministic and Worst-Case Analysis," *IEEE/ACM Transactions on Audio, Speech, and Language Processing*, vol. 24, no. 2, pp. 300–315, Feb. 2016.
- [13] G. W. Elko, "Differential Microphone Arrays," in *Audio Signal Processing for Next-Generation Multimedia Communication Systems*, Y. Huang and J. Benesty, Eds., pp. 11–65. Kluwer Academic Publishers, Boston, 2004.
- [14] J. Benesty and J. Chen, *Study and Design of Differential Microphone Arrays*, Number Volume 6 in Springer Topics in Signal Processing. Springer, Heidelberg; New York, 2013.
- [15] C. Pan, J. Chen, and J. Benesty, "Theoretical Analysis of Differential Microphone Array Beamforming and an Improved Solution," *IEEE/ACM Transactions on Audio, Speech, and Language Processing*, vol. 23, no. 11, pp. 2093–2105, Nov. 2015.
- [16] Y. Buchris, I. Cohen, and J. Benesty, "On the Design of Time-Domain Differential Microphone Arrays," *Applied Acoustics*, vol. 148, pp. 212–222, may 2019.
- [17] G. Huang, J. Benesty, and J. Chen, "On the Design of Frequency-Invariant Beampatterns With Uniform Circular Microphone Arrays," *IEEE/ACM Transactions on Audio, Speech, and Language Processing*, vol. 25, no. 5, pp. 1140–1153, May 2017.
- [18] J. Lovatello, A. Bernardini, and A. Sarti, "Steerable Circular Differential Microphone Arrays," in *European Signal Processing Conference (EUSIPCO)*. Sep. 2018, pp. 11–15, IEEE.
- [19] G. Huang, J. Chen, and J. Benesty, "On the Design of Differential Beamformers with Arbitrary Planar Microphone Array Geometry," *The Journal of the Acoustical Society of America*, vol. 144, no. 1, pp. EL66–EL70, July 2018.
- [20] F. Borra, A. Bernardini, F. Antonacci, and A. Sarti, "Efficient implementations of first-order steerable differential microphone arrays with arbitrary planar geometry," *IEEE/ACM Transactions on Audio, Speech, and Language Processing*, vol. 28, pp. 1755–1766, 2020.
- [21] F. Borra, A. Bernardini, F. Antonacci, and A. Sarti, "Uniform Linear Arrays of First-Order Steerable Differential Microphones," *IEEE/ACM Transactions on Audio, Speech, and Language Processing*, vol. 27, no. 12, pp. 1906–1918, Dec. 2019.
- [22] G. Huang, I. Cohen, J. Benesty, and J. Chen, "Kronecker product beamforming with multiple differential microphone arrays," in *2020 IEEE 11th Sensor Array and Multichannel Signal Processing Workshop (SAM)*, 2020, pp. 1–5.
- [23] M. Brandstein and D. Ward, Eds., *Microphone Arrays: Signal Processing, Techniques and Applications*, Digital Signal Processing. Springer, Berlin, 2001.
- [24] A. Bernardini, F. Antonacci, and A. Sarti, "Wave Digital Implementation of Robust First-Order Differential Microphone Arrays," *IEEE Signal Processing Letters*, vol. 25, no. 2, pp. 253–257, Feb 2018.
- [25] T. I. Laakso, V. Valimaki, M. Karjalainen, and U. K. Laine, "Splitting the unit delay [fir/all pass filters design]," *IEEE Signal Processing Magazine*, vol. 13, no. 1, pp. 30–60, 1996.

### List of typos:

- In the published version of the paper, equation (1) contained a typo in the exponents of the exponentials of the DMA unit steering vector. Therefore in the present postprint version of the paper we corrected it as follows:

$$\mathbf{d}_k(\omega, \theta) = \left[ e^{j\bar{\omega}_k \cos(\theta - \psi_{k,1})}, \dots, e^{j\bar{\omega}_k \cos(\theta - \psi_{k,M_k})} \right]^T.$$

Moreover we slightly rephrased the first paragraph of Section 2 and the sentences after equation (1) for the sake of coherence.

- In the published version of the paper, equation (4) contained a typo in the exponents of the exponentials of the virtual array steering vector. Therefore in the present postprint version of the paper we corrected it as follows:

$$\mathbf{a}(\omega, \theta) = \left[ e^{j\omega \frac{u_{1,x} \cos \theta + u_{1,y} \sin \theta}{c}}, \dots, e^{j\omega \frac{u_{K,x} \cos \theta + u_{K,y} \sin \theta}{c}} \right]^T. \quad (1)$$

Moreover we slightly rephrased the first paragraph of Subsection 2.2 for the sake of coherence.

We would like to highlight the fact that the aforementioned typos were not present in the implementation code. It follows that the simulation results presented in Section 4 are not affected by such typos.